JCAMECH

Vol. 51, No. 1, June 2020, pp 81-90
DOI: 10.22059/jcamech.2020.299581.493

Thermoelastic response of a rotating hollow cylinder based on generalized model with higher order derivatives and phase-lags

A. Soleiman [a,b,*], *Ahmed E. Abouelregal* [a,c], *K. M. Khalil* [a,b] *and M. E. Nasr* [a,b]

[a] *Department of Mathematics, College of Science and Arts, Jouf University, Gurayat, Saudi Arabia*
[b] *Department of Mathematics, Faculty of Science, Benha University, Benha 13518, Egypt*
[c] *Department of Mathematics, Faculty of Science, Mansoura University, Mansoura 35516, Egypt*

ARTICLE INFO

Article history:
Received: 16 March 2020
Accepted: 22 May 2020

Keywords:
Thermoelasticity
Higher-Order
Phase-lags
Rotation
Hollow cylinder

ABSTRACT

The present work treats with a novel generalized model of higher order derivatives heat conduction. Using Taylor series expansion, the Fourier law of heat conduction is advanced by introducing different phase lags for the heat flux and the temperature gradient vectors. Based on this new model, the thermoelastic behavior of a rotating hollow cylinder is analyzed analytically. The governing differential equations are solved in a numerical form using the Laplace transform technique. Numerical calculations are displayed tables and graphs to clarify the effects of the higher order and the rotation parameters. Finally, the results obtained are verified with those in previous literature.

1. Introduction

Generalized thermoelastic models have been developed with the aim of eliminating the contradiction in the infinite velocity of heat propagation inherent in the classical dynamical coupled thermoelasticity theory [1]. In these generalized models, the basic equations include thermal relaxation times and they are of hyperbolic type [2-5]. Furthermore, Tzou [6-8] established the dual-phase-lag heat conduction theory by including two different phase-delays correlating with the heat flow and temperature gradient. Chandrasekharaiah [9] introduced a generalized model improved from the heat conduction model established by Tzou [7, 8]. For details about the physical significance of these models, see, for example [9-19]. As applications of thermoelasticity, Banerjee et al. [20] studied thermoelastic instability in lubricated sliding between solid surfaces. Also, in [21] Wong et al investigated the residual stress measurement by means of the thermoelastic effect. Furthermore, some studies related to a thick walled structure were investigated by Nejad and others [22-26].

Recently, Chiriţă et al. [27, 28] investigated the high-order and time differential dual-phase-lag thermoelastic models for deformable conductors. Abouelregal [29] derived new modified models of generalized thermoelasticity. More recently, Abouelregal et al. studied generalized thermoelastic-diffusion model with higher-order fractional time-derivatives and four-phase-lags in [30].

This paper is devoted to introduce a novel generalized model of higher order derivatives heat conduction and two phase-lags extending Tzou [8]. In this model, the Fourier law of heat conduction is replaced using Taylor series expansions introducing[1] two different phase lags for the heat flux vector and the temperature gradient and keeping the terms up with suitable higher orders.

Based on this model, we have discussed the thermoelastic responses in an isotropic rotating hollow cylinder with constant angular velocity. We used the Laplace transform method to obtain the analytic solutions. The solutions for the field variables are obtained numerically using the numerical Laplace inversion technique. Finally, the results are analyzed in different tables and graphs. Furthermore, the results obtained are verified with those in previous literature.

2. Thermoelastic model with two-phase-lags of high-order (HDPL- Model)

W We know that, the classical Fourier's law [10, 11] which is given by

$$\vec{q}(x,t) = -K\,\nabla\theta(x,t)\,. \tag{1}$$

Here, $\vec{q}(x,t)$ is the heat flux vector, $\theta = T - T_0$ denotes the varying temperature; T is the absolute temperature above the

* Corresponding Author. Tel.: +966559150980;
Email Address: amrsoleiman@yahoo.com

reference temperature T_0 and K denotes the thermal conductivity.

Cattaneo and Vernotte [31, 32] has suggested a thermal wave model with a single phase τ_q of the heat flux as:

$$\vec{q}(x,t+\tau_q) = -K\nabla\theta(x,t) \tag{2}$$

Recently, Tzou [6-8] has proposed a dual-phase-lag model in the following form:

$$\vec{q}(x,t+\tau_q) = -K\nabla\theta(x,t+\tau_\theta) \tag{3}$$

where τ_θ is the phase lag of the temperature gradient. This modification aim to study the effect of microstructural interactions along with the fast transient effects

Dealing in particular with complex biological systems involving several energy carriers, special thermal lagging phenomena have to be taken into account, which further raises the differential orders of the mixed-derivative and the time derivative in the dual-phase-lag equation. Therefore, we introduce a new model that obtained by expanding Eq. (3) in terms of Taylor's series with respect to time and keeping the terms up to specific orders in τ_q and τ_θ of a heat conduction without energy dissipation that includes higher time differential and two phase-lags:

$$\left(1+\sum_{k=1}^{m}\frac{\tau_q^k}{k!}\frac{\partial^k}{\partial t^k}\right)\vec{q} = -K\left(1+\sum_{k=1}^{n}\frac{\tau_\theta^k}{k!}\frac{\partial^k}{\partial t^k}\right)\nabla\theta. \tag{4}$$

The energy balance equation without heat source is given by [10, 11]

$$\rho C_E\frac{\partial\theta}{\partial t}+\gamma T_0\frac{\partial}{\partial t}\left(div\,\vec{u}\right) = -div\,\vec{q}, \tag{5}$$

Where $\gamma = (3\lambda+2\mu)\alpha_t$ denotes the stress temperature modulus, in which α_t means the thermal expansion coefficient, λ,μ are Lamé's constants, C_E represents the specific heat at constant strain, $\vec{u}$ is the displacement vector, ρ is the density of the medium.

Consequently, from Eqs. (4) and (5), we get

$$\left(1+\sum_{k=1}^{m}\frac{\tau_q^k}{k!}\frac{\partial^k}{\partial t^k}\right)\left[\rho C_E\frac{\partial\theta}{\partial t}+\gamma T_0\frac{\partial}{\partial t}\left(div\vec{u}\right)\right] = K\left(1+\sum_{k=1}^{n}\frac{\tau_\theta^k}{k!}\frac{\partial^k}{\partial t^k}\right)\nabla^2\theta \tag{6}$$

This equation define a novel generalized model of higher order derivatives heat conduction and we denoted by HDPL – model. Furthermore, from which we derived special cases, as limited cases, for different sets of values of phase-lags τ_q and τ_θ as follows:

- The classical thermoelasticity theory (CTE) [1] is given when $\tau_q = \tau_\theta = 0$,
- Lord-Shulman theory of thermoelasticity (LS) [2] is obtained when $\tau_q > 0, \tau_\theta = 0$, and $m = 1$.
- The generalized theory with phase-lags (DPL) [8] theory is given by setting $\tau_q \ge \tau_\theta > 0$, and $m = 2, n = 1$.

Finally, the additional basic equations of motion for a homogeneous and isotropic thermoelastic solid are

$$\sigma_{ij} = 2\mu e_{ij} + \delta_{ij}\left[\lambda e_{kk} - \gamma\theta\right] \tag{7}$$

$$2e_{ij} = u_{j,i} + u_{i,j}, \tag{8}$$

$$\sigma_{ij,i} + F_i = \rho\ddot{u}_i, \tag{9}$$

where F_i is the component of the external body forces.

3. Application of HDPL Model.

In this section, we apply our modified model to a homogeneous thermo-homogeneous solid that occupies an infinitely long hollow circular cylinder region for an inner radius a and an outer radius b. Also, we consider that the cylinder rotates uniformly with angular velocity $\vec{\Omega} = \Omega\vec{n}$, where $\vec{n}$ is a unit vector representing the direction of the axis of rotation. We shall use the cylindrical system of coordinates (r,Θ,z) with the z-axis that coincides with the cylinder axis (see Figure 1).

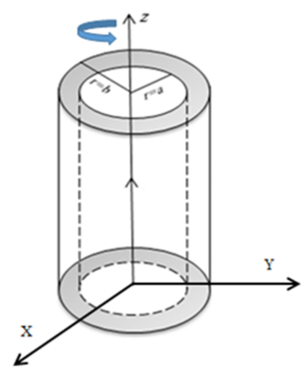

Figure 1. Schematic diagram for the infinitely hollow cylinder.

Assuming that the initial state of the medium is quiescent and that the outer surface of the cylinder is traction free and subjected to a harmonic varying heat, while the inner surface is thermally insulated and also traction free. Due to radial symmetry of the problem, all the considered fields are functions of r and t only. Hence the components of $\vec{u}$ has the form $u_r = u(r,t), u_\Theta = 0, u_z = 0$.

Also, the strain components become

$$e_{rr} = \frac{\partial u}{\partial r}, e_{\Theta\Theta} = \frac{u}{r}, e_{zz} = e_{r\Theta} = e_{rz} = e_{\Theta z} = 0 \tag{10}$$

The cubic dilatation e has the form

$$e = \frac{\partial u}{\partial r}+\frac{u}{r} = \frac{1}{r}\frac{\partial(ru)}{\partial r} \tag{11}$$

The radial stress σ_{rr} and hoop stress $\sigma_{\Theta\Theta}$ given in Eq. (7) are obtained by

$$\sigma_{rr} = 2\mu\frac{\partial u}{\partial r} + \lambda\left(\frac{\partial u}{\partial r} + \frac{u}{r}\right) - \gamma\theta$$
$$\sigma_{\Theta\Theta} = 2\mu\frac{u}{r} + \lambda\left(\frac{\partial u}{\partial r} + \frac{u}{r}\right) - \gamma\theta \quad (12)$$

In view of Eq. (9), the equation of motion in the absence of external body forces and in the presence of rotation take the form [33-35]

$$\frac{\partial\sigma_{rr}}{\partial r} + \frac{1}{r}(\sigma_{rr} - \sigma_{\Theta\Theta}) = \rho\frac{\partial^2 u}{\partial t^2} + \rho\left\{\left[\vec{\Omega}\times\left(\vec{\Omega}\times\vec{u}\right)\right]_r + \left[\vec{\Omega}\times\dot{\vec{u}}\right]_r\right\} \quad (13)$$

If the rotation vector $\vec{\Omega} = (0,0,\Omega)$, then we get

$$\left\{\left[\vec{\Omega}\times\left(\vec{\Omega}\times\vec{u}\right)\right]_r + \left[\vec{\Omega}\times\dot{\vec{u}}\right]_r\right\} = -\Omega^2 u \quad (14)$$

From which together with Eqs. (12), the motion equation (13) becomes

$$(\lambda+2\mu)\left[\frac{\partial}{\partial r}\left(\frac{\partial u}{\partial r} + \frac{u}{r}\right)\right] - \gamma\frac{\partial\theta}{\partial r} = \rho\frac{\partial^2 u}{\partial t^2} - \rho\Omega^2 u \quad (15)$$

In view of Eq. (6), the modified equation of heat conduction with higher-order time-derivatives and phase lags can be written as

$$\left(1 + \sum_{k=1}^{m}\frac{\tau_q^k}{k!}\frac{\partial^k}{\partial t^k}\right)\left[\rho C_E\frac{\partial\theta}{\partial t} + \gamma T_0\frac{\partial e}{\partial t}\right] = K\left(1 + \sum_{k=1}^{n}\frac{\tau_\theta^k}{k!}\frac{\partial^k}{\partial t^k}\right)\nabla^2\theta. \quad (16)$$

To solve the problem, we use the following non-dimensional parameters

$$\{r',u'\} = c_0\eta\{r,u\},\ \{t',\tau_q',\tau_\theta'\} = c_0^2\eta\{t,\tau_q,\tau_\theta\},$$
$$\theta' = \frac{\gamma\theta}{\lambda+2\mu},\ \sigma_{ij}' = \frac{\sigma_{ij}'}{\lambda+2\mu},\ \eta = \frac{\rho C_E}{K}, c_0 = \sqrt{\frac{\lambda+2\mu}{\rho}}, \quad (17)$$
$$\Omega' = \frac{\Omega}{c_0^2\eta}$$

Using Eq. (17), the non-dimensional form of Eqs. (12), (15) and (16) are reduced to

$$\frac{\partial e}{\partial r} - \frac{\partial\theta}{\partial r} = \frac{\partial^2 u}{\partial t^2} - \Omega^2 u \quad (18)$$

$$\left(1 + \sum_{k=1}^{m}\frac{\tau_q^k}{k!}\frac{\partial^k}{\partial t^k}\right)\left[\frac{\partial\theta}{\partial t} + \varepsilon\frac{\partial e}{\partial t}\right] = \left(1 + \sum_{k=1}^{n}\frac{\tau_\theta^k}{k!}\frac{\partial^k}{\partial t^k}\right)\nabla^2\theta. \quad (19)$$

$$\sigma_{rr} = \left(\frac{\beta^2-2}{\beta^2}\right)e + \frac{2}{\beta^2}\frac{\partial u}{\partial r} - \theta$$
$$\sigma_{\Theta\Theta} = \left(\frac{\beta^2-2}{\beta^2}\right)e + \frac{2}{\beta^2}\frac{u}{r} - \theta \quad (20)$$

where

$$\beta^2 = \frac{\lambda+2\mu}{\mu},\ \varepsilon = \frac{\gamma^2 T_0}{\rho C_E(\lambda+2\mu)},\ \nabla^2 = \frac{\partial^2}{\partial r^2} + \frac{1}{r}\frac{\partial}{\partial r} \quad (21)$$

For convenience and clarity, we have dropped the primes in the above equations. In this problem, we assume that the medium initially is at rest, so that the initial conditions are

$$u(r,t) = \frac{\partial u(r,t)}{\partial t} = 0,\ \theta(r,t) = \frac{\partial\theta(r,t)}{\partial t} = 0 \ \text{ at } \ t=0 \quad (22)$$

Also, we consider the outer surface of the hollow cylinder is loaded thermally by a harmonically varying heat and the inner surface is thermally insulated [31-38]. So that

$$\frac{\partial\theta(a,t)}{\partial t} = 0,\ \ \theta(b,t) = G(t) = \theta_1\cos(\omega t) \quad (23)$$

where θ_1 is a constant and ω is the angular frequency of thermal vibration. Note that for a thermal shock problem, we put $\omega = 0$ and for a harmonic varying heat we take $\omega > 0$.

Furthermore, the radial stress component at inner and outer surface of the hollow cylinder are stress-free. Mathematically, these can be written as:

$$\sigma_{rr}(a,t) = 0, \quad \sigma_{rr}(b,t) = 0 \quad (24)$$

4. Transform solution

Applying the Laplace transform method, defined by the following formula

$$\bar{f}(r,s) = \int_0^\infty f(r,t)e^{-st}dt,\ \mathrm{Re}(s) > 0$$

into Eqs. (18)-(20) and using homogeneous initial conditions (22), we obtain

$$\frac{d\bar{e}}{dr} - \frac{d\bar{\theta}}{dr} = [s^2 - \Omega^2]\bar{u} \quad (25)$$

$$\ell_q\bar{\theta} + \varepsilon\ell_q\bar{e} = \ell_\theta\nabla^2\bar{\theta} \quad (26)$$

$$\bar{\sigma}_{rr} = \left(\frac{\beta^2-2}{\beta^2}\right)\bar{e} + \frac{2}{\beta^2}\frac{d\bar{u}}{dr} - \bar{\theta}$$
$$\bar{\sigma}_{\Theta\Theta} = \left(\frac{\beta^2-2}{\beta^2}\right)\bar{e} + \frac{2}{\beta^2}\frac{\bar{u}}{r} - \bar{\theta} \quad (27)$$

where the parameters ℓ_q and ℓ_θ are given by

$$\ell_q = s\left(1 + \sum_{k=1}^{m}\frac{\tau_q^k}{k!}s^k\right), \quad \ell_\theta = \left(1 + \sum_{k=1}^{n}\frac{\tau_\theta^k}{k!}s^k\right). \quad (28)$$

Multiplying both sides by r and then using the operator $\frac{1}{r}\frac{d}{dr}$ to both sides of Eq. (25), yields

$$\nabla^2\bar{e} - \nabla^2\bar{\theta} = [s^2 - \Omega^2]\bar{e} \quad (29)$$

Hence, we can write Eqs. (26) and (29) in the following forms

$$\nabla^2 \bar{e} - \alpha_1 \bar{e} = \nabla^2 \bar{\theta} \tag{30}$$

$$\alpha_2 \bar{e} = \ell_\theta \nabla^2 \bar{\theta} - \ell_q \bar{\theta} \tag{31}$$

where

$$\alpha_1 = s^2 - \Omega^2, \ \alpha_2 = \varepsilon \ell_q \tag{32}$$

Elimination of $\bar{e}$ or $\bar{\theta}$ from Eqs. (30) and (31), yields

$$\left[\nabla^4 - A\nabla^2 + B\right](\bar{\theta}, \bar{e}) = 0 \tag{33}$$

which can be written in the form

$$\left[(\nabla^2 - m_1^2)(\nabla^2 - m_2^2)\right](\bar{\theta}, \bar{e}) = 0\,, \tag{34}$$

where $m_i^2 \, (i = 1,2)$ are the square roots of the following characteristic equation

$$\begin{gathered} m^4 - Am^2 + B = 0, \\ A = \frac{\ell_q}{\ell_\theta} + \alpha_1 + \frac{\alpha_2}{\ell_\theta}, \ B = \alpha_1 \frac{\ell_q}{\ell_\theta} \end{gathered} \tag{35}$$

Thus, we have

$$\begin{aligned} \bar{\theta} &= \sum_{i=1}^{2} \left[A_i(s) I_0(m_i r) + B_i(s) K_0(m_i r)\right] \\ \bar{e} &= \sum_{i=1}^{2} \left[A_i'(s) I_0(m_i r) + B_i'(s) K_0(m_i r)\right] \end{aligned} \tag{36}$$

where A_i, A_i', B_i, B_i' are arbitrary constants, and $I_0(m_i r), K_0(m_i r)$ indicate the modified Bessel functions of first and second kind of order zero, respectively.

Substituting the expressions of $\bar{e}$ and $\bar{\theta}$ into Eq. (30), we get

$$A_i' = \frac{m_i^2}{(m_i^2 - \alpha_1)} A_i\,, \ B_i' = \frac{m_i^2}{(m_i^2 - \alpha_1)} B_i \tag{37}$$

From which together Eq. (36), we obtain

$$\bar{e} = \sum_{i=1}^{2} \left[\frac{m_i^2}{(m_i^2 - \alpha_1)}\right] \left[A_i(s) I_0(m_i r) + B_i(s) K_0(m_i r)\right] \tag{38}$$

By using Eqs. (11) and (38), we have

$$\bar{u} = \sum_{i=1}^{2} k_i \left[A_i(s) I_1(m_i r) - B_i(s) K_1(m_i r)\right] \tag{39}$$

where $k_i = \dfrac{m_i}{(m_i^2 - \alpha_1)}, \ i = 1,2$.

From which , we get

$$\frac{d\bar{u}}{dr} = \sum_{i=1}^{2} k_i \left[\begin{aligned} &\left(m_i I_0(m_i r) - \frac{1}{r} I_1(m_i r)\right) A_i(s) \\ &+ \left(m_i K_0(m_i r) + \frac{1}{r} K_1(m_i r)\right) B_i(s) \end{aligned}\right] \tag{40}$$

In addition, the thermal stresses that appeared in Eqs (27) after using Eqs. (36)-(40), can be expressed as

$$\bar{\sigma}_{rr} = \sum_{i=1}^{2} \left[\begin{aligned} &\left(L_i I_0(m_i r) - \frac{2k_i}{\beta^2 r} I_1(m_i r)\right) A_i(s) \\ &+ \left(L_i K_0(m_i r) + \frac{2k_i}{\beta^2 r} K_1(m_i r)\right) B_i(s) \end{aligned}\right] \tag{41}$$

$$\bar{\sigma}_{\Theta\Theta} = \sum_{i=1}^{2} \left[\begin{aligned} &\left(R_i I_0(m_i r) + \frac{2k_i}{\beta^2 r} I_1(m_i r)\right) A_i(s) \\ &+ \left(R_i K_0(m_i r) - \frac{2k_i}{\beta^2 r} K_1(m_i r)\right) B_i(s) \end{aligned}\right] \tag{42}$$

where

$$L_i = m_i k_i - 1, \ R_i = L_i - \left(\frac{2}{\beta^2}\right) m_i k_i \tag{43}$$

Now, the boundary conditions (23) and (24), after applying Laplace transform, become

$$\begin{gathered} \frac{d\bar{\theta}(a,s)}{dr} = 0, \ \bar{\theta}(b,s) = \bar{G}(s), \\ \bar{\sigma}_{rr}(a,s) = 0, \ \bar{\sigma}_{rr}(b,s) = 0 \end{gathered} \tag{44}$$

Hence, one obtains the following system of equations

$$\sum_{i=1}^{2} \left[A_i(s) I_0(bm_i) + B_i(s) K_0(bm_i)\right] = \frac{\theta_1 s}{s^2 + \omega^2} = \bar{G}(s) \tag{45}$$

$$\sum_{i=1}^{2} m_i \left[A_i(s) I_1(am_i) - B_i(s) K_1(am_i)\right] = 0 \tag{46}$$

$$\sum_{i=1}^{2} \left[\begin{aligned} &\left(L_i I_0(bm_i) - \frac{2k_i}{b\beta^2} I_1(bm_i)\right) A_i(s) \\ &+ \left(L_i K_0(bm_i) + \frac{2k_i}{b\beta^2} K_1(bm_i)\right) B_i(s) \end{aligned}\right] = 0 \tag{47}$$

$$\sum_{i=1}^{2} \left[\begin{aligned} &\left(L_i I_0(am_i) - \frac{2k_i}{a\beta^2} I_1(am_i)\right) A_i(s) \\ &+ \left(L_i K_0(am_i) + \frac{2k_i}{a\beta^2} K_1(am_i)\right) B_i(s) \end{aligned}\right] = 0 \tag{48}$$

Finally, from the above system we can determine the parameters $A_i, B_i; i = 1,2$ in the Laplace transform domain and hence the physical fields of the medium.

To have the solutions of the studied fields in the physical domain, we use a proper and effective numerical method depending on a Fourier series expansion [39]. In this method, any function $\bar{\mathrm{M}}((r,s)$ in the Laplace domain can be reversed to the time domain as

$$\mathrm{M}(r,t)=\frac{e^{ct}}{t}\left[\frac{1}{2}\bar{\mathrm{M}}(r,c)+\mathrm{Re}\sum_{n=1}^{m}\bar{\mathrm{M}}\left(r,c+\frac{in\pi}{t}\right)(-1)^{n}\right] \quad (49)$$

where m is a finite number of terms, Re is the real part and i is imaginary number unit. For faster convergence, numerous numerical experiments have shown that the value of c satisfies the relation $ct \cong 4.7$ [40].

5. Numerical results and verification

The purpose of this section is to explain and validate the results obtained in the preceding sections. First, we present the numerical results. For the numerical calculations, we take the value of the Copper material at $T_0 = 293K$ as [41]

$\lambda = 7.76\times10^{10}\,kg\,m^{-1}s^{-2}$, $\mu = 3.86\times10^{10}\,kg\,m^{-1}s^{-2}$,

$\rho = 8954 kg\,m^{-3}, K = 386 W\,m^{-1}K^{-1}$, $C_E = 3.381\,J\,kg\,K^{-1}$,

$\varepsilon = 0.0168$, $\beta = 2$.

The results are presented in Tables (1-4) and graphically in Figs. (2-13) at different radius of r. The calculations were carried out for the wide range of $r(1 \le r \le 2)$ at $t = 0.25$, when $\tau_\theta = 0.01$, and $\tau_q = 0.05$. For all numerical calculations Mathematica programming Language has been used. The numerical calculation is made for three cases.

5.1. Influence of the higher expansion order on the physical fields

In this subsection, the distributions of the field variables for different models of thermoelasticity (CTE, LS and DPL) together with advanced model with higher order derivatives and phase-lags (HDPL) are investigated. The results are represented in Tables (1-4) for the field quantities to various high orders m, n and the radial space $(1 \le r \le 2)$. These tables show that the physical quantities depend not only on the time t and radial space r, but also on the higher order parameters m and n. Also, the obtained result emphasize that it is enough to put $m = 5, n = 4$ for accurate results and avoid problems appeared in $m = 6, n = 5$.

Table 1: The effect of the higher orders m, n on the temperature θ

r	CTE	LS	DPL	HDPL			
				$m=3, n=2$	$m=4, n=3$	$m=5, n=4$	$m=6, n=5$
١,0	0.305711	0.532222	0.850326	0.52203	0.360126	0.489421	1.06253
١,١	0.319761	0.671237	0.992053	0.332727	0.288425	0.443584	0.76669
١,٢	0.361214	0.731887	0.502415	0.234998	0.307326	0.394841	0.356385
١,٣	0.413965	0.620799	0.094974	0.178295	0.330725	0.316891	-0.00364938
١,٤	0.468569	0.465051	0.197464	0.302032	0.40926	0.314741	-0.0692643
١,٥	0.519865	0.363448	0.49747	0.408833	0.505694	0.393735	0.169652
١,٦	0.566563	0.33929	0.6431	0.494043	0.606478	0.528741	0.567197
١,٧	0.604767	0.472027	0.627477	0.592666	0.674253	0.654101	0.896148
١,٨	0.711018	0.836705	0.71126	0.796985	0.824512	0.852235	1.13584
١,٩	0.887379	0.944645	0.809355	0.898992	0.934807	0.979204	1.14883
٢,٠	1.02386	1.02386	1.02386	1.02386	1.02386	1.02386	1.02386

Table 1 indicates the variation of temperature θ, for different models of thermoelasticity. Through the tables provided, we note that the variations of temperature are observed to be sensitive to the parameters of the higher order of the time derivatives up to $m = 5, n = 4$. The hyperbolic models of thermoelasticity (LS, DPL, and HDPL) give significantly different results than the parabolic theory (CTE). From the considerd table, we observe that the variation of temperature θ in all models increases with increasing the radial space r. This observation is consistent with the theoretical results acquired by other investigations [41]

Table 2: Effect of the higher order Taylor expansions on the displacement u

r	CTE	LS	DPL	HDPL			
				$m=3, n=2$	$m=4, n=3$	$m=5, n=4$	$m=6, n=5$
١,0	-0.0557927	-0.0126134	-0.0190267	-0.0683857	-0.0501125	-0.0406079	-0.0464675
١,١	-0.0328045	-0.0371059	-0.0243073	-0.00720522	-0.0150947	-0.0183316	-0.025794
١,٢	-0.0274212	-0.0317353	-0.0275871	-0.0251629	-0.0280746	-0.0306697	-0.0314931
١,٣	-0.0256367	-0.0312268	-0.0279166	-0.0275804	-0.0251464	-0.0276678	-0.0256251
١,٤	-0.0219002	-0.0282666	-0.0221688	-0.0175345	-0.0205197	-0.0211585	-0.018912
١,٥	-0.0193115	-0.0189656	-0.0182362	-0.0212196	-0.0199479	-0.0190718	-0.0178769
١,٦	-0.0183508	-0.0181401	-0.0192836	-0.0192833	-0.019006	-0.0187075	-0.0179485
١,٧	-0.0196293	-0.0167242	-0.0203583	-0.0190149	-0.0205648	-0.0208137	-0.0200927
١,٨	0.0212953	0.0109871	0.00954462	0.0119057	0.0126755	0.0117521	0.0117625
١,٩	0.111882	0.103462	0.103564	0.103796	0.104345	0.103811	0.10327
٢.0	0.208193	0.200462	0.201248	0.200488	0.200891	0.200608	0.199946

Also from the results it is clear that the higher order of the derivatives have a very significant effect on the temperature distributions and this corresponds to Chiriţă [27, 28].

The variation of the displacement u in the context of four models of thermoelasticity is given in Table 2. It was found that the values of the parameters m and n play a significant role in changing the displacement value. As seen from Table 2, the displacement attains minimum value on the boundary at $r = 1$ and increase slowly in the range $1 \le r \le 2$. Also, about the range $1 \le r \le 1.4$, the displacement profile is smaller for the LS model than that of the CTE and DPL models, which is smaller than the HDPL model. Finally, we observe that when the values of m and n increase, the greatest value of the displacement increases up to $m = 5, n = 4$.

Table 3: Effect of the higher order Taylor expansions on the radial stress σ_{rr}

r	CTE	LS	DPL	HDPL			
				$m = 3, n = 2$	$m = 4, n = 3$	$m = 5, n = 4$	$m = 6, n = 5$
1.0	0	0	0	0	0	0	0
1.1	-0.195781	-0.491026	-0.921674	-1.03614	-0.486435	-0.401592	-0.862641
1.2	-0.375033	-0.752093	-0.540409	0.174679	-0.198044	-0.24329	-0.46809
1.3	-0.375467	-0.34253	-0.12942	-0.302845	-0.392918	-0.378636	-0.165331
1.4	-0.440827	-0.257707	-0.296361	-0.303101	-0.389771	-0.336101	0.078903
1.5	-0.507874	-0.182567	-0.547599	-0.365978	-0.517476	-0.380149	-0.0953917
1.6	-0.580765	-0.0848539	-0.654435	-0.638556	-0.711309	-0.566882	-0.587671
1.7	-0.683925	-0.325567	-0.651546	-0.729134	-0.885124	-0.799271	-1.04021
1.8	0.251986	0.437809	0.395603	0.262734	0.128493	0.131935	-0.143866
1.9	0.115415	0.173823	0.252157	0.124739	0.0598786	0.0225756	-0.141156
2.5	0	0	0	0	0	0	0

Table 4: Effect of the higher order Taylor expansions on the hoop stress $\sigma_{\Theta\Theta}$

r	CTE	LS	DPL	HDPL			
				$m = 3, n = 2$	$m = 4, n = 3$	$m = 5, n = 4$	$m = 6, n = 5$
1.0	-0.188419	-0.274206	-0.436551	-0.303768	-0.211954	-0.27045	-0.559903
1.1	-0.277617	-0.603106	-0.971686	-0.690412	-0.397485	-0.434189	-0.8307
1.2	-0.38402	-0.759951	-0.537444	-0.0440035	-0.268506	-0.336262	-0.430251
1.3	-0.408584	-0.498151	-0.127581	-0.255647	-0.375487	-0.362732	-0.0950172
1.4	-0.465833	-0.375393	-0.258464	-0.311989	-0.40998	-0.336278	0.0642484
1.5	-0.523171	-0.282279	-0.531449	-0.397661	-0.521178	-0.396154	-0.14114
1.6	-0.58208	-0.2203	-0.657527	-0.575343	-0.667745	-0.556456	-0.585714
1.7	-0.652963	-0.406008	-0.648382	-0.66924	-0.788883	-0.735911	-0.977089
1.8	-0.219317	-0.193212	-0.152401	-0.260504	-0.341429	-0.353908	-0.633585
1.9	-0.340527	-0.343075	-0.236361	-0.344699	-0.395037	-0.436074	-0.602928
2.5	-0.432618	-0.435453	-0.43518	-0.435419	-0.435389	-0.435481	-0.435698

Tables 3 and 4 show the variations of thermal stresses σ_{rr} and $\sigma_{\Theta\Theta}$ against the radial distance r for different high expansion orders m and n. Specially, Table 3 shows that the radial stress σ_{rr} has an initial point at $r = 1$ and $r = 2$ that coincides with a zero value, which agrees completely with the boundary conditions. From these Tables, it is shown that the magnitude of thermal stresses for the HDPL model is smaller than that of the other models about $1.6 \le r \le 2$ and different on the other range of r. From the results, it is also, clear that the distributions of the various fields increase and decrease with the higher orders of differentiation unless they reach the degree of stability, and this is consistent with what Abouelregal reached [29, 30].

5.2 The effect of rotation on the physical fields

This subsection is devoted to discus how the field variables differ with different values of the rotation parameter Ω under the generalized modfied model with higher order and phase lags (HDPL). In this case, we +take $m = 3$ and $n = 2$, and other parameters such τ_q and τ_θ remain constants ($\tau_q = 0.1$ and $\tau_\theta = 0.05$). The results are graphically illustrated in Figs. 2-5. We take $\Omega = 1,3$ for the rotating case and for the non-rotating, we put $\Omega = 0$.

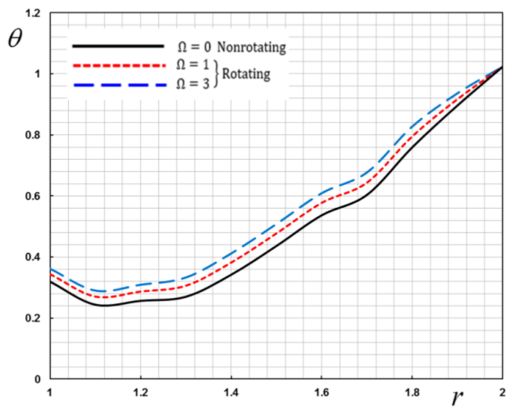

Figure 2. The effect of rotation Ω on the temperature θ

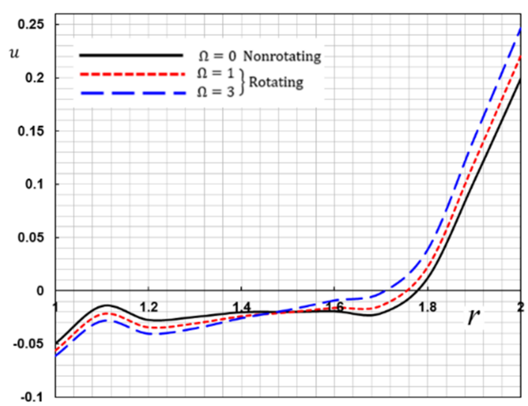

Figure 3. The effect of rotation Ω on the displacement u .

It is evident from Fig. 2 that the rotation parameter Ω has clearly effect on the temperature θ. The direction of temperature change increses monotony with increasing radial distance r. It is also manifested from the figure that increasing values of Ω are having an increasing effect on the values of temperature variations. This observation is consistent with the theoretical results acquired by other studies [35, 41].

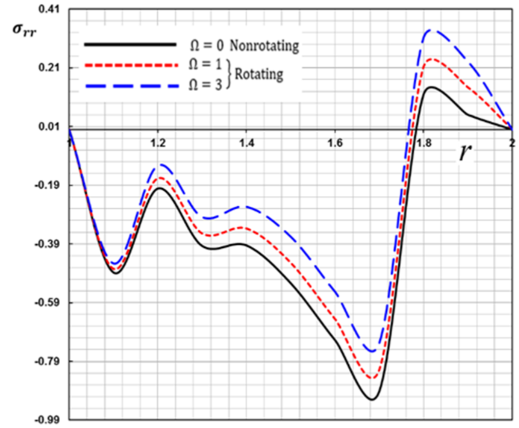

Figure 4. The effect of rotation Ω on the radial stress σ_{rr} .

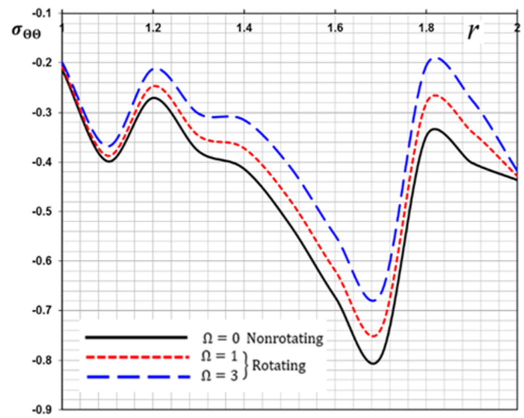

Figure 5. The effect of rotation Ω on the hoop stress $\sigma_{\Theta\Theta}$.

In Fig. **3**, the variation of the radial displacement u decreases with increasing the value of Ω for $0 < r < 1.48$ and increases on $1.5 < r < 2$.

Finally, Figures 4-5 show that the variation of thermal stresses σ_{rr} and $\sigma_{\Theta\Theta}$ against the radial distance r for different values of the rotation Ω. It is noticed that, when we increase the value of Ω the behavour of the stresses increase clearly. On the other hand, Figures 4 shows that the radial stress σ_{rr} has an initial point at $r = 1$ and $r = 2$ that coincides with a zero value, which is in quite good agreement with the boundary conditions.

5.3 The effect of thermal vibration on the physical fields

Here, we study the variations of the physical fields with different values of the thermal vibration ω under the dual-phase-lag model. Other parameters such as the rotating parameter Ω, phase-lag of the heat flux τ_q and the phase-lag of temperature gradient τ_θ remain constant. The numerical results are obtained and presented graphically in Figs. 6-9. We put $\omega = 2,3,4$ for the harmonic case and $\omega = 0$ for the thermal shock case.

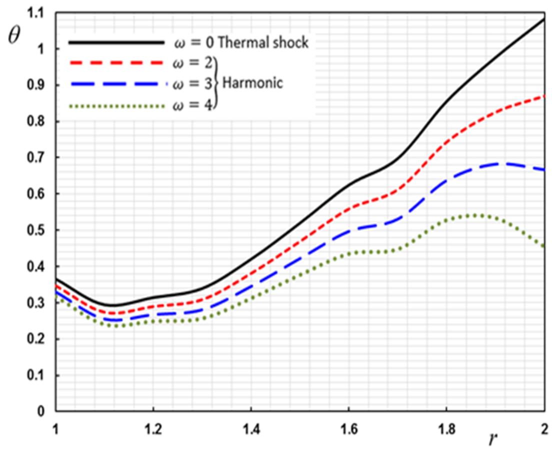

Figure 6. The effect of thermal vibration ω on the temperature θ .

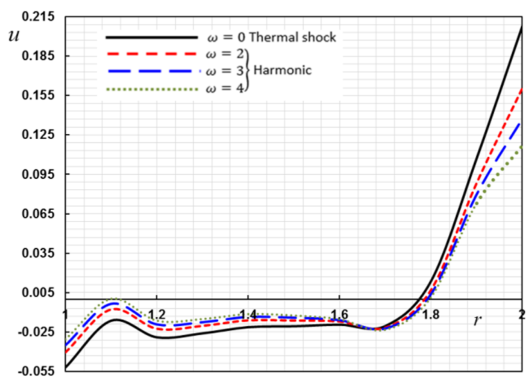

Figure 7. The effect of thermal vibration ω on the displacement u .

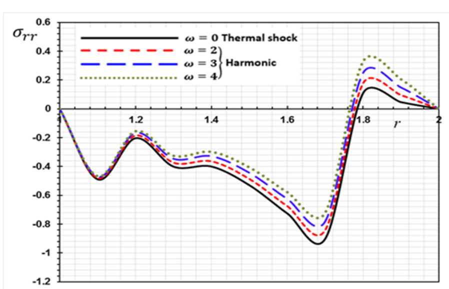

Figure 8. The effect of thermal vibration ω on the radial stress σ_{rr}

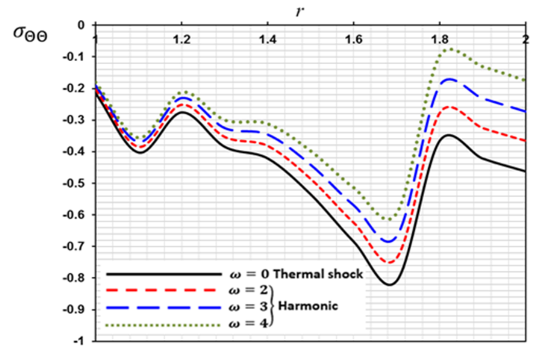

Figure 9. The effect of thermal vibration ω on the hoop stress $\sigma_{\Theta\Theta}$

In Fig. **6**, we observe that the variation of temperature decreases for the harmonic case and increases for the thermal shock. This means that, the value of temperature decreses with increasing the value of thermal vibration. This remark is consistent with the obtained results attained by other investigations [38]. In view of Fig. **7**, we conclude that the change of the radial displacement u increases with increasing the value of ω for $0 \le r \le 1.68$ and decreases on $1.7 \le r \le 2$.

Finally, Figures **8-9** show that the variation of thermal stresses σ_{rr} and $\sigma_{\Theta\Theta}$ against the radial distance r for different values of the rotation ω Also, the change of thermal stresses increase with increasing the value of the thermal vibration. On the other hand, Figures **8** shows that the radial stress σ_{rr} has an initial point that coincides with a zero value, which is consistent with the applied boundary conditions.

5.4 The effect of the time on the physical fields

This section is devoted to show the effect of the time t on all the field variables. In this case, we take $m = 3$, $n = 2$ and other parameters such τ_q and τ_θ remain constants ($\tau_q = 0.1$ and $\tau_\theta = 0.05$), together with $\Omega = \omega = 1$. For a comparison of the results, the temperature, the displacement, and thermal stresses σ_{rr} and $\sigma_{\Theta\Theta}$ are presented in Figs. 10-13. It is seen from the figures that these distributions are very sensitive with the time instant t It is also clear from the figures (12) and (13) that the behavior of the thermal stresses are the most affected by the change of time [14, 15]. The temperature also increases with the increase of time to a certain range and then gradually decreases again with the passage of time.

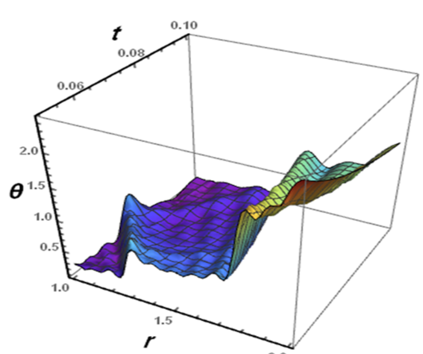

Figure 10. The temperature θ with different time.

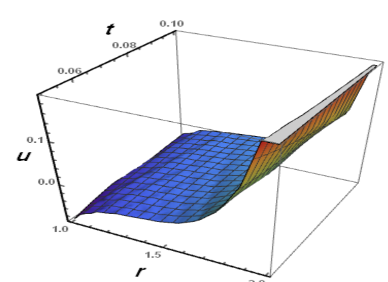

Figure 11. The displacement u with different time.

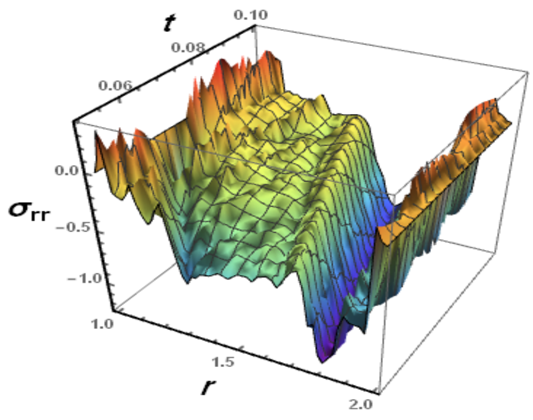

Figure 12. The radial stress σ_{rr} with different time.

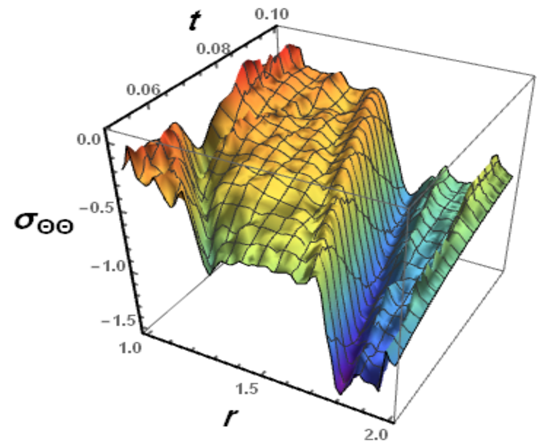

Figure 13. The hoop stress $\sigma_{\Theta\Theta}$ with different time.

6. Conclusion

A novel generalized model of higher order derivatives heat conduction is investigated. In view of this model, the distributions of the physical fields for a rotating hollow cylinder are discused. Additionally, the distrbutions for the classical theory of coupled thermoelasticity (CTE), and the hyperbolic models of thermoelasticity (LS, DPL) are obtained. Numerical simulation results yield the following conclusions:

- The classical thermoelasticity theory (CTE) and the hyperbolic models (LS, DPL) are obtained as special cases of the present model.
- Acoording to Tables (1-4) and Figs. (10-13), we conclude that the physical quantities depend not only on the time t and radial space r, but also on the higher expansion order parameters m and n
- In view of Figs. (2-5), the field variables differ with different values of the rotation parameter Ω under the dual-phase-lag model.
- According to the results shown in Figs. (6-9), we find that the thermoelastic stresses, displacement and temperature have a strong dependency on the thermal vibration parameter.
- It is worth mentioning that these observations above are consistent with the theoretical results obtained by other studies [35, 38-41]

Nomenclature:

λ, μ	Lam´e's constants	K	thermal conductivity
α_t	thermal expansion coefficient	ρ	material density
C_E	specific heat	Q	heat source
$\gamma = (3\lambda + 2\mu)\alpha_t$	thermal coupling parameter	t	the time
T_0	environmental temperature	δ_{ij}	Kronecker's delta function
$\theta = T - T_0$	temperature increment	$\vec{E}$	induced electric field
T	absolute temperature	τ_q	phase lag of heat flux
$\boldsymbol{u}$	displacement vector	τ_θ	phase lag of temperature
$e = \text{div}\,\mathbf{u}$	cubical dilatation	e_{ij}	strain tensor
σ_{ij}	stress tensor	$\boldsymbol{q}$	heat flux vector

Acknowledgments

The authors would like to thank the referees for their valuable suggestions and useful comments which improved this paper.

References

[1] M. Biot, Thermoelasticity and Irreversible Thermodynamics, *Journal of Applied Physics* Vol. 27, No. 3, pp. 240-253, 1956.

[2] H. Lord, Y. Shulman, A generalized dynamical theory of thermoelasticity, *Journal of the Mechanics and Physics of Solids,* Vol. 15, No. 5, pp. 299-309, 1967.

[3] A. E. Green, K. A. Lindsay, Thermoelasticity, *Journal of Elasticity,* Vol. 2, pp. 1-7, 1972.

[4] A. E. Green, P.M. Naghdi, A re-examination of the basic postulates of thermomechanics, *proceedings of the Royal Society of London. Series A,* Vol. 432, pp. 171-194, 1991.

[5] A. E. Green, P. M. Naghdi, Thermoelasticity without energy dissipation, *Journal of Elasticity,* Vol. 31, pp. 189-208, 1993.

[6] D. Y. Tzou, Thermal Shock Phenomena in Solids Under High-Rate Response, *Annual Review of Heat Transfer,* Vol. 4, pp. 111-185, 1992.
[7] D. Y. Tzou, A unified field approach for heat conduction from macro-to micro-scales, *Journal of Heat Transfer,* Vol. 117, No. 1, pp. 8-16, 1995.
[8] D. Y. Tzou, The generalized lagging response in small-scale and high-rate heating, *International Journal of Heat and Mass Transfer,* Vol. 38, No. 17, pp. 3231-3240, 1995.
[9] D. S. Chandrasekharaiah, Hyperbolic thermoelasticity: a review of recent literature, *Applied Mechanics Reviews,* Vol. 51, No. 12, pp. 705-729, 1998.
[10] R. B. Hetnarski, J. Ignaczak, Generalized thermoelasticity, *Journal of Thermal Stresses,* Vol. 22, No. 4-5, pp. 451-476, 1999.
[11] J. Ignaczak, *Generalized thermoelasticity and its applications*, in: R. B. Hetnarski, *Mechanics and Mathematical Methods*, Eds., pp. 279-354, North Holland: Elsevier Science Publications B. v., 1989.
[12] R. Quintanilla, R. Racke, A note on stability in dual-phase-lag heat conduction, *International Journal of Heat and Mass Transfer,* Vol. 49, No. 7-8, pp. 1209-1213, 2006.
[13] R. Quintanilla, R. Racke, Qualitative Aspects in Dual Phase-Lag Heat Conduction, *proceedings of the Royal Society of London. Series A,* Vol. 463, pp. 659-674, 2007.
[14] A. M. Zenkour, A.E. Abouelregal, Effects of phase-lags in a thermoviscoelastic orthotropic continuum with a cylindrical hole and variable thermal conductivity, *Archives of Mechanics,* Vol. 67, No. 6, pp. 457-475, 2015.
[15] A. M. Zenkour, D.S. Mashat, A.E. Abouelregal, The Effect of Dual-Phase-Lag Model on Reflection of Thermoelastic Waves in a Solid Half Space with Variable Material Properties, *Acta Mechanica Solida Sinica,* Vol. 26, pp. 659–670, 2013.
[16] S. Kant, S. Mukhopadhyay, Investigation on effects of stochastic loading at the boundary under thermoelasticity with two relaxation parameters, *Applied Mathematical Modelling,* Vol. 54, pp. 648-669, 2018.
[17] K. Borgmeyer, R. Quintanilla, R. Racke, Phase-Lag Heat Condition: Decay Rates for Limit Problems and Well-Posedness, *Journal of Evolution Equations,* Vol. 14, pp. 863–884, 2014.
[18] Z. Liu, R. Quintanilla, Time Decay in Dual-Phase-Lag Thermoelasticity: Critical Case, *Communications on Pure & Applied Analysis,* Vol. 17, No. 1, pp. 177-190, 2018.
[19] F. L. Guo, G. Q. Wang, G. A. Rogerson, Analysis of thermoelastic damping in micro- and nanomechanical resonators based on dual-phase-lagging generalized thermoelasticity theory, *International Journal of Engineering Science,* Vol. 60, pp. 59-65, 2012.
[20] B. N. Banerjee, R. A. Burton, Thermoelastic instability in lubricated sliding between solid surfaces, *Nature,* Vol. 261, pp. 399–400, 1976.
[21] A. K. Wong, S. A. Dunn, J. G. Sparrow, Residual stress measurement by means of the thermoelastic effect, *Nature,* Vol. 332, pp. 613–615, 1988.
[22] M. Z. Nejad, M. Jabbari, A. Hadi, A review of functionally graded thick cylindrical and conical shells, *Journal of Computational Applied Mechanics,* Vol. 48, No. 2, pp. 357-370, 2017.
[23] M. Hosseini, M. Shishesaz, A. Hadi, Thermoelastic analysis of rotating functionally graded micro/nanodisks of variable thickness, *Thin-Walled Structures,* Vol. 134, pp. 508-523, 2019.
[24] M. Z. Nejad, N. Alamzadeh, A. Hadi, Thermoelastoplastic analysis of FGM rotating thick cylindrical pressure vessels in linear elastic-fully plastic condition, *Composites Part B: Engineering,* Vol. 154, pp. 410-422, 2018.
[25] A. Hadi, A. Rastgoo, N. Haghighipour, A. Bolhassani, Numerical modelling of a spheroid living cell membrane under hydrostatic pressure, *Journal of Statistical Mechanics: Theory and Experiment,* Vol. 2018, No. 8, pp. 083501, 2018.
[26] M. Gharibi, M. Z. Nejad, A. Hadi, Elastic analysis of functionally graded rotating thick cylindrical pressure vessels with exponentially-varying properties using power series method of Frobenius, *Journal of Computational Applied Mechanics,* Vol. 48, No. 1, pp. 89-98, 2017.
[27] S. Chiriţă, High-order effects of thermal lagging in deformable conductors, *International Journal of Heat and Mass Transfer,* Vol. 127, No. Part C, pp. 965-974, 2018.
[28] S. Chiriţă, On the time differential dual-phase-lag thermoelastic model, *Meccanica,* Vol. 52, pp. 349–361, 2017.
[29] A. E. Abouelregal, Modified fractional thermoelasticity model with multi-relaxation times of higher order: application to spherical cavity exposed to a harmonic varying heat, *Waves in Random and Complex Media*, 17 Jun, 2019.
[30] A. E. Abouelregal, M. A. Elhagary, A. Soleiman, K. M. Khalil, Generalized thermoelastic-diffusion model with higher-order fractional time-derivatives and four-phase-lags, *Mechanics Based Design of Structures and Machines*, pp. 1-18, 2020.
[31] C. Cattaneo, A Form of Heat-Conduction Equations Which Eliminates the Paradox of Instantaneous Propagation, *Comptes Rendus,* Vol. 247, pp. 431-433, 1958.
[32] P. Vernotte, Les paradoxes de la theorie continue de l'equation de la chaleur, *Comptes Rendus,* Vol. 246, pp. 3154-3155, 1958.
[33] N. S. Clarke, J. S. Burdess, Rayleigh Waves on a Rotating Surface, *Journal of Applied Mechanics,* Vol. 61, No. 3, pp. 724-726, 1994.
[34] M. A. A. Abdou, M. I. A. Othman, R. S. Tantawi, N. T. Mansour, Effect of Rotation and Gravity on Generalized Thermoelastic Medium with Double Porosity under L-S Theory, *Journal of Materials Science & Nanotechnology,* Vol. 6, No. 3, pp. 304-317, 2018.
[35] A. Gunghas, R. Kumar, S. Deswal, K. K. Kalkal, Influence of Rotation and Magnetic Fields on a Functionally Graded Thermoelastic Solid Subjected to a Mechanical Load, *Journal of Mathematics,* Vol. 2019, pp. 1-16, 2019.
[36] A. E. Abouelregal, On Green and Naghdi Thermoelasticity Model without Energy Dissipation with Higher Order Time Differential and Phase-Lags, *Journal of Applied and Computational Mechanics,* Vol. 6, No. 3, pp. 445-456, 2020.
[37] A. E. Abouelregal, Two-temperature thermoelastic model without energy dissipation including higher order time-derivatives and two phase-lags, *Materials Research Express,* Vol. 6:116535, No. 11, 2019.
[38] A. M. Zenkour, A. E. Abouelregal, Nonlocal thermoelastic vibrations for variable thermal conductivity nanobeams due to harmonically varying heat, *Journal of Vibroengineering,* Vol. 16, No. 8, pp. 3665-3678, 2014.
[39] G. Honig, U. Hirdes, A method for the numerical inversion of Laplace Transform, *Journal of Computational and Applied Mathematics,* Vol. 10, pp. 113-132, 1984.
[40] D. Y. Tzou, Experimental support for the lagging behavior in heat propagation, *Journal of thermophysics and heat transfer,* Vol. 9, No. 4, pp. 686-693, 1995.
[41] M. I. A. Othman, A. E. Abouelregal, Magnetothermoelstic analysis for an infinite solid cylinder with variable thermal conductivity due to harmonically varying heat, *Microsystem Technologies,* Vol. 23, No. 12, pp. 5635–5644, 2017.